Journal of Computational Neuroscience 3, 179–198 (1996)

Distributed Processing on the Basis of Parallel and Antagonistic Pathways Simulation of the Femur-Tibia Control System in the Stick Insect

A.E. SAUER
FB Biologie, Universität Kaiserslautern, 67653 Kaiserslautern, Germany
asauer@rhrk.uni-kl.de

R.B. DRIESANG
Institut für Physiologie, Leipziger Straße 44, 39120 Magdeburg, Germany

A. BÜSCHGES AND U. BÄSSLER
FB Biologie, Universität Kaiserslautern, 67653 Kaiserslautern, Germany

Received September 11, 1995; Revised December 4, 1995; Accepted December 21, 1995

Action Editor: A. Borst

Abstract. In inactive stick insects, sensory information from the femoral chordotonal organ (fCO) about position and movement of the femur-tibia joint is transferred via local nonspiking interneurons onto extensor and flexor tibiae motoneurons. Information is processed by the interaction of antagonistic parallel pathways at two levels: (1) at the input side of the nonspiking interneurons and (2) at the input side of the motoneurons. We tested by a combination of physiological experiments and computer simulation whether the known network topology and the properties of its elements are sufficient to explain the generation of the motor output in response to passive joint movements, that is resistance reflexes. In reinvestigating the quantitative characteristics of interneuronal pathways we identified 10 distinct types of nonspiking interneurons. Synaptic inputs from fCO afferents onto these interneurons are direct excitatory and indirect inhibitory. These connections were investigated with respect to position and velocity signals from the fCO. The results were introduced in the network simulation. The motor output of the simulation has the same characteristics as the real system, even when particular types of interneurons were removed in the simulation and the real system.

Keywords: reflex pathway, neuronal network, simulation, parliamentary principle, neural basis of behavior

Introduction

During the past two decades, investigation of the neural basis of behavior has led to detailed insight into the function of nervous systems in vertebrates and invertebrates. Considerable knowledge has been accumulated about the activity of identified neurons in neuronal networks involved, for example, in rhythm generation, posture control, and visual orientation in invertebrates (locust flight: Pearson and Ramirez, 1992; Wolf, 1991; stomatogastric nervous system: Harris-Warrick et al., 1992b; fly orientation: Egelhaaf and Borst, 1993; cockroach escape circuit: Ritzmann and Pollack, 1990; insect posture control and reflex generation: Bässler, 1993; Burrows, 1992). In some systems, the knowledge of premotor neural activity appears to be qualitatively sufficient to explain the generation of a particular behavior

(Pearson and Ramirez, 1992; Harris-Warrick et al., 1992a).

It is particularly from studies on reflex generation that very detailed knowledge about the neuronal circuits processing mechanosensory signals has become available (e.g., Bässler, 1993; Burrows and Laurent, 1989; Pearson, 1995). These studies revealed that in both vertebrates and in invertebrates, proprioceptive signals are processed in complex pathways, called parallel distributed processing (PDP; McClelland and Rumelhart, 1988; Anastasio and Robinson, 1990; Lockery and Kristan, 1990a, b). The information processed by each of the individual parallel pathways supports a certain feature of the generated motor output and these features add up at the motoneuronal level. These studies led to the concept that simple motor patterns or reflexes are generated by dedicated neuronal networks (Burrows, 1992). However, recent findings have indicated that this view of sensory-motor processing might be too simplistic even in the case of relatively simple behavior (Bässler et al., 1986; Zecevic et al., 1989; Morton and Chiel, 1994). More recent investigations on sensory-motor processing in vertebrates and invertebrates have shown that not each of the involved parallel pathways supports the generated motor output and some even oppose the overall motor output. In this case the motor output is the difference between the influences from supporting and from opposing pathways (crayfish uropod reflexes: Nagayama and Hisada, 1987; leech bending reflex: Lockery and Kristan, 1990a, b; stick insect and locust joint control: Büschges, 1990; Büschges and Wolf, 1995; cat: Osborn and Popelle, 1992). In the leech, this kind of information processing has been termed *distributed processing*. In the stick insect and locust, it was called *parliamentary principle* (Bässler, 1993; Büschges and Wolf, 1995).

The neuronal network that governs the femur-tibia (FT) joint of the stick insect middle leg stabilizes in the standing animal the actual FT angle (Bässler, 1983, 1993). Particularly in this network, the interaction of parallel antagonistic pathways has now been shown on two neuronal levels: (1) nonspiking interneurons either support or oppose the generation of the resistance reflex in the excitatory extensor motoneurons (Büschges, 1990); (2) some of these nonspiking interneurons (E4, E5) themselves receive excitatory and inhibitory input induced by the same stimulus modality (velocity of a flexion movement) (Sauer et al., 1995).

From the findings mentioned above two questions arise: (1) Do all nonspiking interneurons receive excitatory as well as inhibitory input, and is this network topology sufficient for generating the different dependencies of the membrane potential on fCO movement parameters? (2) Is the current knowledge about the organization of the femur-tibia control loop sufficient to explain the generation of the resistance reflex?

We therefore set out to simulate the FT control network based on the experimental data obtained from its neuronal elements. In doing so we first had to reinvestigate the physiology of the neuronal elements of the femur-tibia control network, since important information such as the velocity dependency of interneuronal responses was still lacking. We then simulated the neuronal network of the stick insect femur-tibia control loop based on these quantitative experimental data with a network simulator using realistic neurons (Grimm and Sauer, 1995; Bergdoll and Koch, 1995). In the present paper, we will provide evidence that the simulation of the femur-tibia control network based on parallel antagonistic pathways resembled to a high degree the neuronal activity during resistance reflexes in the inactive stick insect *in vivo*. Since the characteristics of the femur-tibia control system are the cause of catalepsy (Bässler, 1983), these results trace back the behavior of catalepsy to the properties and connections of the neurons involved. In addition a success of the simulation could give rise to new hypotheses on the generation of state dependent alterations in the motor output of joint control systems, that have been repeatedly described (for review see Pearson, 1993).

Methods

The experiments were carried out on adult female stick insects *Carausius morosus* Brunner and *Cuniculina impigra* Redtenbacher (syn. *Baculum impigrum* Brunner) from the colonies at the University of Kaiserslautern.

Preparation and Intracellular Recordings

Intracellular recordings were performed as described in detail in previous studies (Büschges, 1990; Sauer et al., 1995). The animals were restrained dorsal side up on a foam platform and dissected from dorsal. The mesothoracic ganglion was fixed on a wax-coated ganglion holder. The activity of interneurons was recorded

in the dorso-lateral neuropil region of the mesothoracic ganglion. Thin-walled glass microelectrodes (wpi), filled with 4% Lucifer Yellow (tip solution) and 1M LiCl (shaft solution; electrode resistance: 40–70 MΩ) were used for intracellular recordings from interneurons and motoneurons. The activity of nonspiking interneurons was recorded in both *Cuniculina impigra* and *Carausius morosus* and the neurons were identified by both morphological and physiological properties (Büschges, 1990; Driesang and Büschges, 1993). There were no major qualitative differences in the physiological properties between interneurons of both species. The physiological results presented here are based on a total number of six recordings from E1, three from E2, 13 from E3, 74 from E4, 12 from E5, 10 from E6, four from E7, 15 from I1, six from I2, six from I4. For the evaluation of the quantitative data, three recordings from interneuron E1, two from E2, five from E3, 17 from E4, three from E5, six from E6, four from E7, four from I1, two from I2, three from I4 were used.

The fCO was mechanically stimulated with ramp-and-hold or sinusoidal stimuli with amplitudes of 100 μm or 400 μm and stimulus velocities between 0.067 mm/s and 9.4 mm/s (13.4°/s to 1481.5°/s in *Carausius* and 6.7°/s to 1240.7°/s in *Cuniculina*) (Weiland and Koch, 1987). The activity of the extensor motoneurons was either recorded extracellularly with a hook electrode (Schmitz et al., 1991) from nerve F2, which innervates the extensor tibiae muscle, or intracellularly from the neuropil region of the motoneurons.

Electrical Stimulation of fCO Afferents

These experiments were carried out on adult female *Cuniculina impigra*. The preparation was essentially the same as described above, with parts of the dorsal cuticle of coxa and trochanter removed. The levator trochanteris muscle and parts of the protractor and retractor coxae muscles were cut distally. Two hooked micro-needles were used as bipolar stimulation electrodes on nerve F1, which contains the afferents of the fCO (for details see Sauer et al., 1995). These electrodes were insulated from the saline by a mixture of silicone oil and paraffin oil. For stimulation, rectangular current pulses of 0.1 ms duration and variable amplitude were used (generated by a H. Sachs Stimulator T via an isolator, ISOflex, A.M.P.I). The resulting compound spike of fCO afferents was recorded extracellularly from the nervus cruris prior to its entrance into the ganglion. The threshold amplitude of the stimulus for eliciting a compound spike in the nervus cruris was set 1.0 T. The amplitudes of the stimuli were normalized to this threshold.

Simulation Software

The simulations were performed with the program BioSim 4.3 (Bergdoll and Koch, 1995), which was controlled for sequential simulations and the definition and application of input functions by the simulation tool SUPERVISOR (Wendel, 1993). Details of the hardware and software requirements for the simulation tool are described by Sauer et al. (1995).

Definition of Neurons and Connections in BioSim

A single neuron consists of a spike generating zone and three dendritic compartments, coupled via a longitudinal resistance. The compartments were defined by the parameters of capacity, leakage, and resting potential. Neurons can be coupled via chemical synapses connecting the spike generating zone of the presynaptic compartment with one of the compartments of the postsynaptic neuron. An axon is not simulated.

Spikes were generated by setting the Na^+ conductance, after reaching the spike threshold, to a constant, user defined value. The resulting current was computed in relation to the momentary membrane potential. The Na^+ channel was closed after a fixed time interval. The K^+ conductance was increased delayed, even in a fixed sequence of time. Nonspiking neurons were defined by setting the parameter "conductance" of the Na^+ and K^+ channel to a value of zero. All parameters settings refer to a membrane area of 1 cm^2.

Regression Analysis

The regression lines for neuronal responses to fCO stimuli against stimulus velocity were calculated by using the statistic package of the program Plotit 3.0 for Windows (ICS). For comparison of the motoneuronal response in different animals, the responses of individual animals were normalized (response to maximal stimulus velocity = 1).

Results

Characteristics of the Neuronal Elements of the Femur-Tibia Control Network

A schematic wiring diagram of the neuronal network controlling the FT joint in the inactive animal, as it is

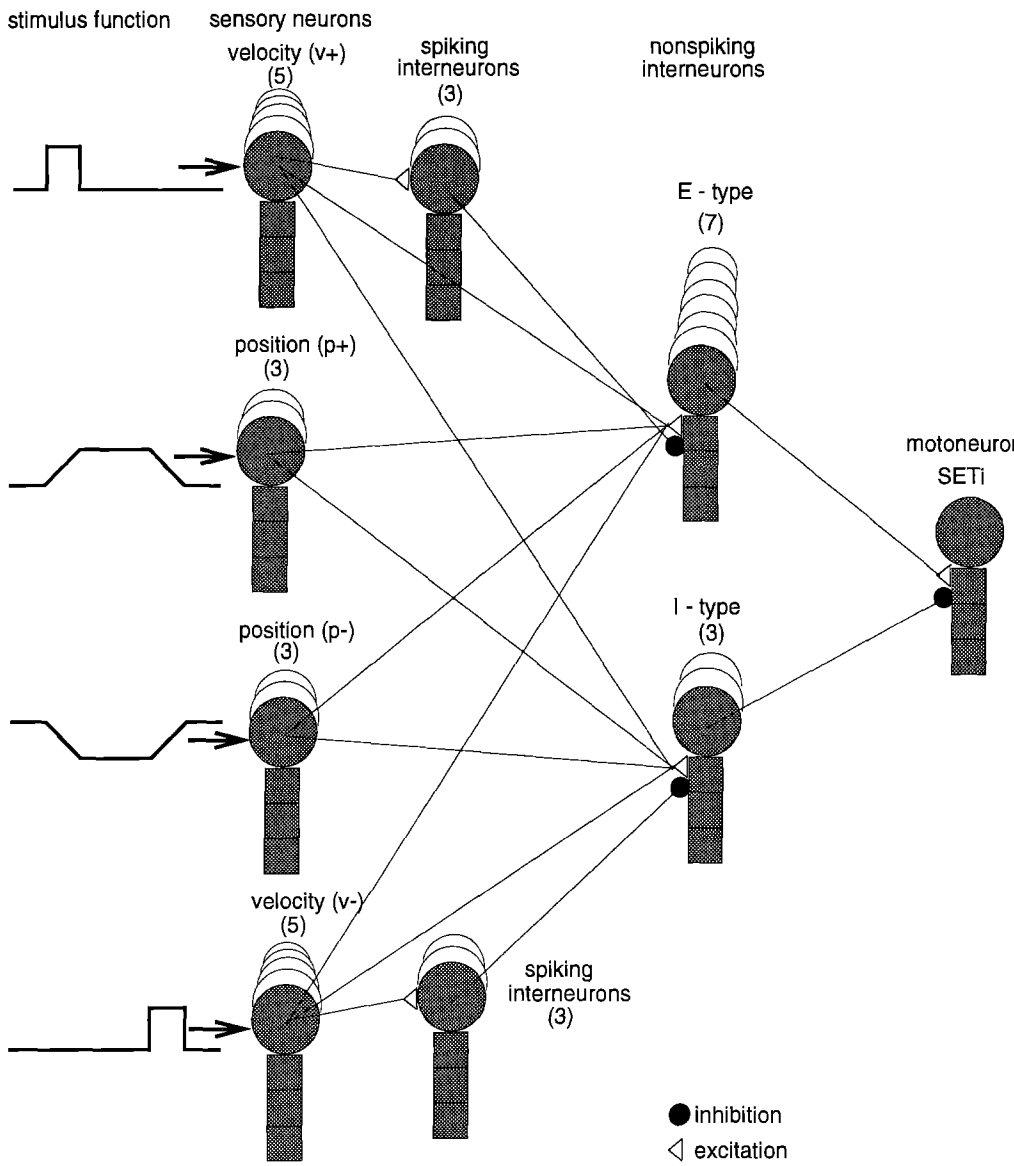

Figure 1. Wiring diagram of the network used in the simulation. As an example the connections to an E-type interneuron are shown (for simulation of an I-type interneuron, the connection to the motoneuron is inhibitory). The inputs to the different types of sensory neurons show the time course of the applied current that simulated the response characteristic of the different sensory neurons. The neurons are drawn as circles, representing the spike generating compartment (SGC in Table 1) with three connected squares symbolizing the passive dendritic compartments. —◁ excitatory synapse; —● inhibitory synapse.

known in previous and the present investigation (see the introduction) and as it was realized in the simulation, is shown in Fig. 1. A set of afferent neurons of the femoral chordotonal organ (fCO) is stimulated by a simulated joint movement, that is, a ramp and hold stimulus applied to the receptor apodeme of the fCO. The sensory information is transmitted via direct connections on nonspiking and spiking interneurons. The nonspiking interneurons themselves receive additional inhibitory input from the spiking interneurons. The nonspiking interneurons again provide either excitatory or inhibitory drive to the extensor motoneurons,

Table 1. Parameters used for the simulation of sensory neurons (P = position sensitive, V = velocity sensitive), spiking interneurons (SN), nonspiking interneurons (NSI), and the motoneuron (SETi). SGC = spike generating compartment. The parameters marked as VARIABLE were used to fit the physiology of the neurons with the physiology of the natural prototype. These parameters are individual for each type of nonspiking interneuron and the motoneuron. The settings of this parameters are given in Fig. 11.

	P-Neurons	V-Neurons	Spiking interneurons (SN)	Nonspiking interneurons (NSI)	Motoneuron [SETi]
Passive parameters					
Leakage conductance [nS]	5	5	5	4	12
Membrane potential [mV]	−55/−50/−41	−60/−55/−50/−40	−65	−40/−38	−47
Membrane capacitance [pF]	200	200	200	200	200
Start potential [mV]	−55/−50/−41	−60/−55/−50/−40	−65	−40/−38	−44
Conductance to SGC/dendrite [nS]	40	40	40	40	20
Channel parameters					
Sodium equilibrium potential [mV]	50	50	50	50	50
Sodium conductance [nS]	800	800	800	0	800
Sodium channel open time [ms]	0.3	0.3	0.3	0	0.3
Potassium equilibrium potential [mV]	−90	−90	−90	−90	−90
Potassium conductance [nS]	320	320	320	0	320
Potassium channel start time [ms]	0.4	0.4	0.4	0	0.4
Potassium channel open time [ms]	3	3	3	0	3
Spike threshold [mV]	−40	−40	−40	0	−40
Synapse Parameters	V-neurons to SN	P-neurons to NSI	V-neurons to NSI	SN to NSI	NSI to motoneuron
Equilibrium potential [mV]/type	50/Na^+	50/Na^+	50/Na^+	−90/K^+	50/NA^+(E) −90/K^+(I)
Conductance [nS]	VARIABLE	VARIABLE	VARIABLE	VARIABLE	VARIABLE
Synaptic delay [ms]	1	6	6	10/15/22	1
Release threshold [mV]	−40	−40	−40	−40	−40
Position on postsynaptic neuron	SGC	Dendrite 1	Dendrite 1	Dendrite 1	SGC

such as the slow extensor tibiae motoneuron (SETi). The activity of SETi results from the interaction of several neuronal pathways.

1. Response Characteristics of the Afferents. fCO sensory neurons measure the parameters position (P), velocity (V) and acceleration (A) of fCO movement for each stimulus direction—elongation (joint flexion) and relaxation (joint extension). Beside these cell types, sensory cells that respond to a combination of these parameters are also known (Hofmann et al., 1985; Hofmann and Koch, 1985; Büschges, 1994). In addition, position-sensitive sensory cells with slow adaptation properties have been identified (Sauer et al., 1995).

The simulation of the afferents has been described in detail by Sauer et al. (1995). However, for better clarity the main aspects of the simulation are shortly presented here again. The afferents were defined as velocity-sensitive or position-sensitive by specific input functions. Passive membrane parameters and channel parameters for these neurons (Table 1) were chosen in a way that spike frequency in response to different holding positions or with different stimulus velocities corresponded to the characteristics of the real neurons. We simulated five velocity-sensitive and three position-sensitive neurons for each stimulus direction with slightly different membrane potentials in the simulation to ensure a homogeneous excitation during the stimulus and range-fractionation of the afferents (see Matheson, 1992).

2. Response Characteristics of the Nonspiking Interneurons. For the simulation of the responses of nonspiking interneurons of type E1, E2, E3, E5, I1,

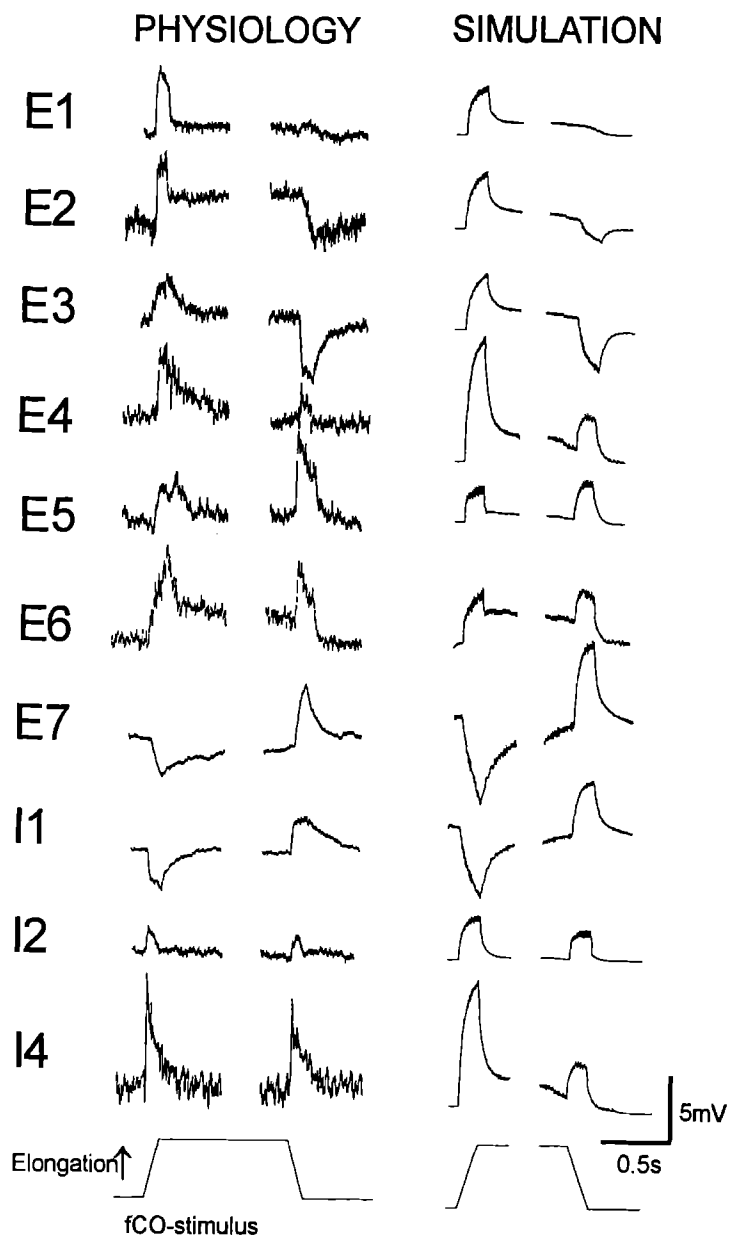

Figure 2. The responses of the 10 types of nonspiking interneurons processing sensory signals from fCO onto extensor motoneurons during resistance reflexes in the stick insect (left side). On the right side the simulated responses of the nonspiking interneurons are shown.

and I2, a quantitative analysis of their response to fCO stimuli was necessary. We recorded the activity of these nonspiking interneurons during ramp-and-hold stimulation of the fCO and evaluated their responses to stimulus velocity and position. Figure 2 shows a summary of the responses of all types of nonspiking interneurons for ramp-and-hold stimulation of the fCO. During these experiments two new types of interneurons were found. The first type of interneuron that provided excitatory synaptic drive to extensor motoneurons, was named E7 and the other, which provided inhibitory drive to extensor motoneurons, was named I4.

The latter type of nonspiking interneuron (I4) (Fig. 3A) was recorded twice in *Carausius morosus* and three times in *Cuniculina impigra*. This type of interneuron provided inhibitory synaptic drive to

extensor motoneurons (Fig. 3B) and excitatory synaptic drive to flexor motoneurons. Hyperpolarizing the neuron did not change SETi discharge rate. Because of its morphological similarity to interneurons of type E4, it was termed I4 (cf. Büschges, 1990; Driesang and Büschges, 1993). In addition, we found that interneurons of type I4 provided excitatory drive to the common inhibitor 1 motoneuron (CI1). Interneurons of type I4 were depolarized during elongation and relaxation of the fCO (Fig. 3C). The latencies of the responses to the different stimulus directions are shown in Table 2. The velocity dependency of the interneuronal response is shown in Fig. 3D for three recordings. Two time constants were detected in the decline of the membrane potential during the holding phase of a ramp-and-hold stimulus. For the recording shown in Fig. 3C

Table 2. Latencies of interneuronal responses to elongation and relaxation stimuli to the fCO.

Neuron type	Latency of response to elongation stimuli [ms]	Latency of response to relaxation stimuli [ms]
E1	7.2 a	b
E2	5.3 a	b
E3	5.2 a	10.5 c
E4	5.0 a	5.4 a
E5	5.2 a	5.6 a
E6	5.8 a	5.9 a
E7	14 c	5.0 a
I1	21 c	7.5 a
I2	21.1 a	8.4 a
I4	6.4 a	8.4 a

a. Excitation, b. no detectable response, c. inhibition.

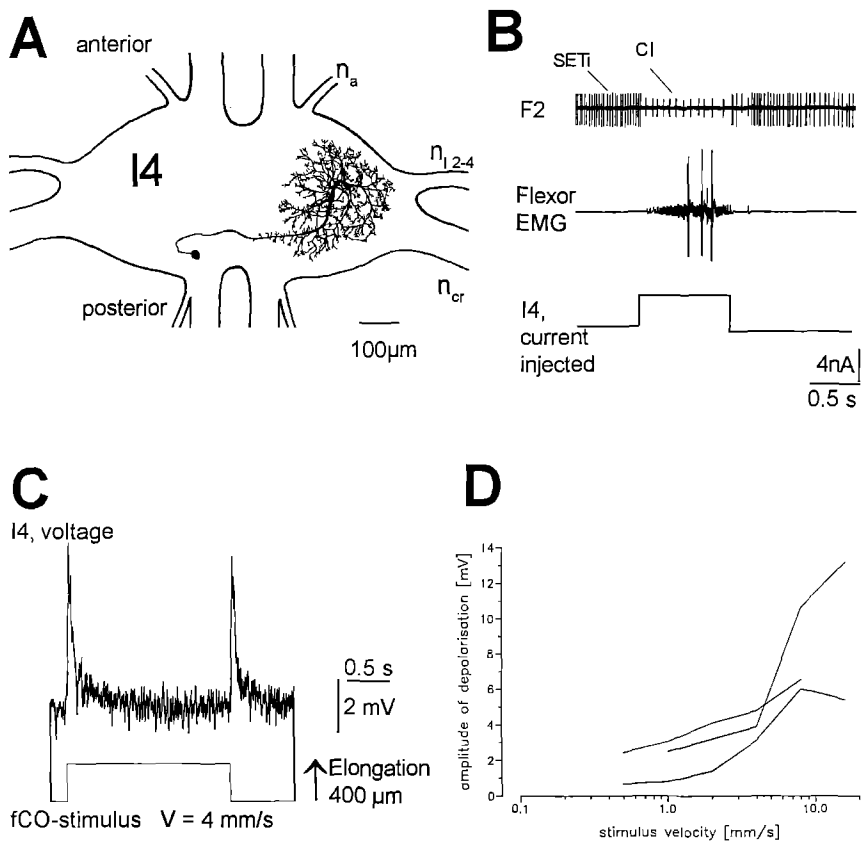

Figure 3. Morphological and physiological properties of nonspiking interneuron type I4. A. Morphology of the interneuron in the mesothoracic ganglion. B. Change in the activity of flexor- and extensor-motoneuron activity in response to injection of depolarizing current into interneuron I4. Note that spontaneous activity of SETi, as visible in the recording from extensor nerve F2 was decreased and the discharge rate of the common inhibitor 1 (CI1) was increased. The electromyogram of the flexor activity shows the activation of different flexor units. C. Response of interneuron I4 to ramp-and-hold stimuli at the fCO. D. Plot of the depolarization amplitude of the membrane potential in interneuron I4 *versus* elongation velocity for three different recordings. The mean values of at least 3 responses in each experiment are given.

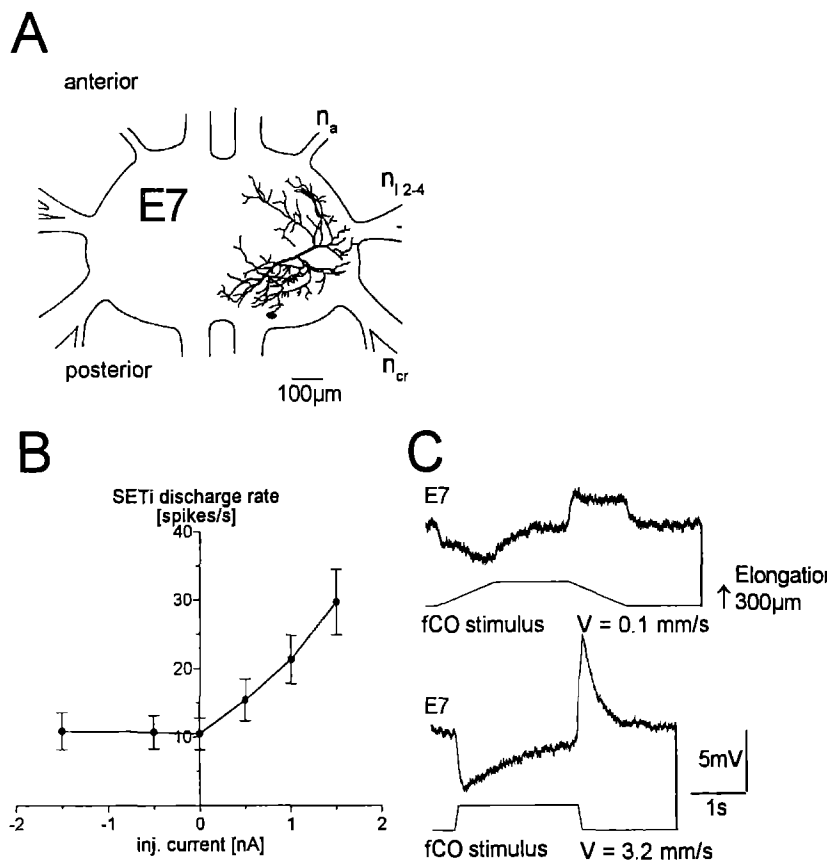

Figure 4. Morphological and physiological properties of a nonspiking interneuron type E7. A. Morphology of the interneuron. B. Relationship between the current injected into interneuron E7 and the mean discharge rate of SETi. C. Response of interneuron E7 to ramp-and-hold stimulation at the fCO for two different stimulus velocities.

$\tau_1 = 21$ ms and $\tau_2 = 221$ ms were calculated from an average over eight ramp-and-hold stimuli in one I4. τ_1 and τ_2 are thus in the same range as those described for interneuron type E4 (Driesang and Büschges, 1993). The membrane potential did not depend from the fCO position. In summary, the responses of I4 to fCO stimuli are very similar to those of E4, but I4 interneurons provide opposite synaptic drive onto extensor motoneurons.

The other type of nonspiking interneuron, type E7, was recorded once in *Cuniculina impigra* and three times in *Carausius morosus*. Its morphology is shown in Fig. 4A. Injecting of depolarizing current increased SETi activity, whereas injection of hyperpolarizing current had no effect (Fig. 4B). Elongation stimuli led to a hyperpolarization of interneuron E7 (for latency see Table 2) and relaxation stimuli depolarized it (Fig. 4C). There was only a small position-sensitive portion of the response in E7. The relationship between the hyperpolarization amplitude and velocity of fCO elongation is shown in Fig. 5A.

3. Simulation of Nonspiking Interneurons. The basis for the simulation of the time course of the membrane potential in the different types of interneurons was the connectivity described for the simulation of the interneuron types E4 and E6 (Sauer et al., 1995). In brief, the simulated nonspiking interneuron received direct excitatory input from six position-sensitive sensory neurons, three of which were sensitive to fCO elongation and three to fCO relaxation. Two sensory neurons of each group showed a slow adaptation with a time constant of 500 ms. They also received direct excitatory inputs from 10 velocity-sensitive units, five sensitive to the velocity of fCO elongation stimuli and five to the relaxation stimulus direction. All interneurons received a delayed inhibitory input from both types of velocity-sensitive units. The inhibition was mediated

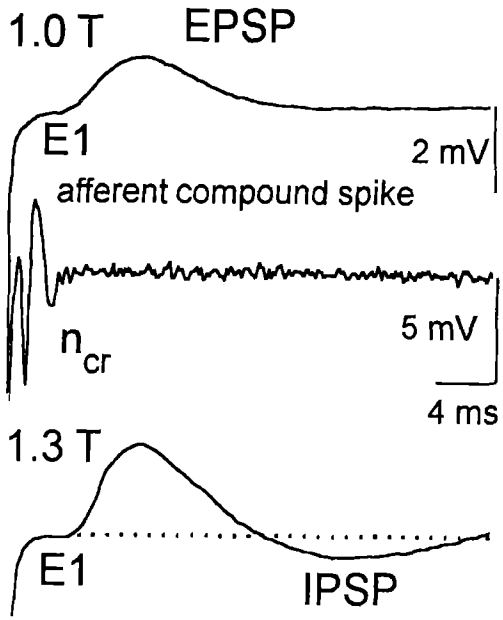

Figure 5. Intracellular recording from a nonspiking interneuron of type E1 in *Cuniculina* during electrical stimulation of the fCO nerve F1. The compound spike of fCO afferents was recorded extracellularly from nervus cruris (n_{cr}). At 1.3 times stimulus threshold (1.3 T) the EPSP in the nonspiking interneuron was followed by an IPSP with a larger latency.

and delayed by a group of six intercalated spiking neurons. This group received excitatory input from the velocity-sensitive neurons. Three of them are sensitive to elongation stimuli and three to relaxation stimuli.

In Sauer et al. (1995), this network topology has been shown for interneurons of type E4 and E6 which receive a net depolarization during fCO stimulation. Before introducing this topology in the simulation of the other interneuronal pathways, we first investigated in detail the synaptic signals received by the other interneurons from fCO afferents during electrical or mechanical stimulation. From these experiments three lines of evidence suggest that the other types of nonspiking interneurons also receive direct excitation and a delayed inhibition induced by the same stimulus parameter.

1. Intracellular recordings from all types of nonspiking interneurons being depolarized during electrical stimulation of the fCO—nerve F1 showed short latency EPSPs at 1.0 T stimulus strength (see Methods) and long latency IPSPs with greater latency at higher stimulus strengths (1.3 T) (Fig. 5).
2. We analyzed the latencies of the responses to ramp-wise stimuli at the fCO (Table 2) in all types of interneurons. The latencies for excitatory synaptic inputs during ramp-and-hold stimulation range from 5.0 to 8.4 ms for all types, except for I2. The latencies for inhibitory synaptic inputs during ramp-wise stimulation of the fCO range from 10.5 to 21 ms (Table 2). Again, this difference in latency indicates that the inhibition is mediated by longer latency pathways and is most likely due to intercalated interneurons.
3. Intracellular recordings from the other nonspiking interneurons revealed excitatory and inhibitory signals from fCO afferents induced by the same stimulus modality, as previously shown for interneurons E4 and E6 by Sauer et al. (1995). The results thus showed that not only E4 and E6 neurons but also the other nonspiking interneurons receive direct excitation and delayed inhibition from fCO afferents.

The situation was different for interneurons receiving a net hyperpolarization during a certain stimulus direction. At the moment we have no evidence that these interneurons also receive excitatory synaptic signals with the stimulus parameter inducing their long latency hyperpolarization. Therefore, we simulated these responses only with disynaptic inhibitory input from fCO afferents (cf. responses of interneurons E7 and I1 to elongation stimuli).

The measured latencies (Table 2) were introduced in the simulation by adjusting the parameter synaptic delay of the excitatory synapses on the nonspiking interneurons to a value of 6 ms and for the inhibitory synapses of the additional group of spiking interneurons onto the nonspiking interneurons to values between 10 and 22 ms (compare with the parameter settings in Table 1). It has to be taken into account that these latency values represent the sum of (1) the mechano-electrical transduction in the fCO neurons, (2) the conduction time from the fCO via the axons of the fCO sensory neurons to the ganglion and (3) the central synaptic delay. The latter is known to be 0.8 to 1.1 ms in the stick insect, as measured for direct excitatory connections between fCO afferents and nonspiking interneurons (Sauer et al., 1995).

4. Simulation of the Quantitative Characteristics of the Interneuronal Response. Is the physiological difference in the types of interneurons due to the relative amounts of excitatory and inhibitory input? The form

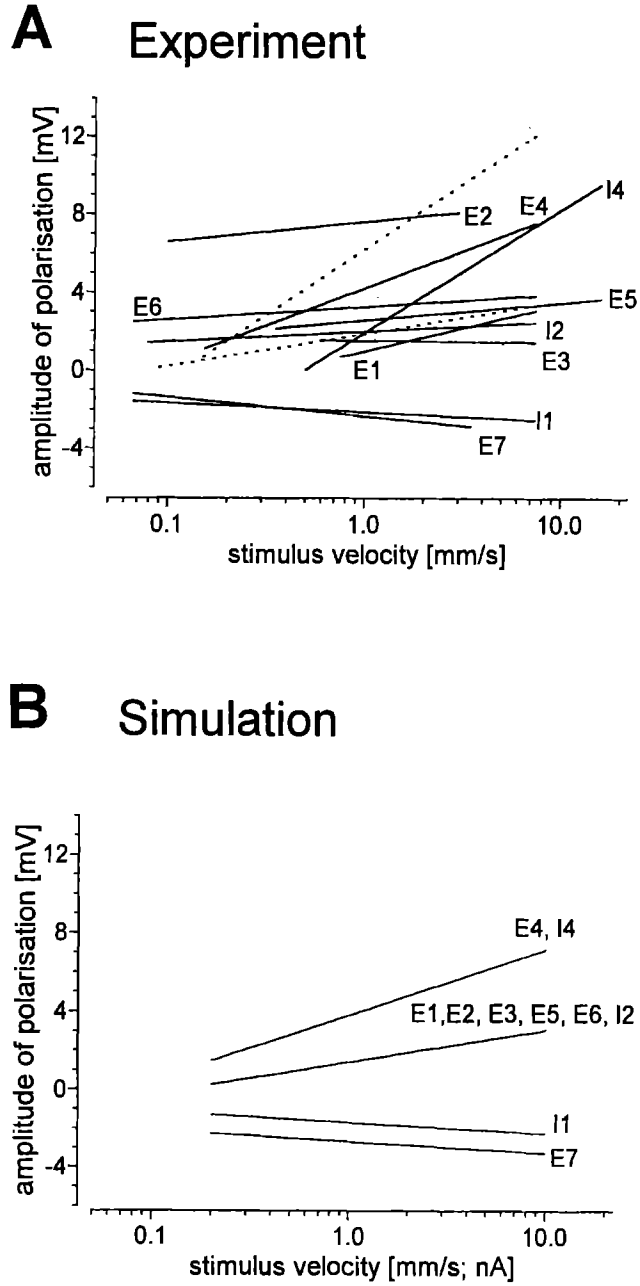

Figure 6. A. Plot of experimental data showing the relationship between amplitude of depolarization and hyperpolarization of membrane potential and stimulus velocity. The regression lines are based on at least two data sets for a certain type of interneuron tested for different stimulus velocities. For interneuron of type E4 the maximum and minimum regression line measured in two different experiments (dotted lines) are given. B. Plot of the simulated data on the amplitude of depolarization or hyperpolarization *versus* stimulus velocity for the nonspiking interneurons. Regression lines with slightly different slopes, as of types E1, E2, E3, E5, E6, and of the types E4, I4, were combined.

of the response (Fig. 2) as well as the relationship between velocity of elongation stimuli and amplitude of depolarization or hyperpolarization differs for different types of nonspiking interneurons. Figure 6A shows the regression lines for the latter relationship in different types of interneurons that were measured during the recordings (see also Büschges, 1990; Driesang and Büschges, 1993; Büschges and Wolf, 1995; Sauer et al., 1995). We simulated the different slopes for the relationship between stimulus velocity and membrane

potential by biasing the excitatory and inhibitory input to the nonspiking interneurons. For example a steep slope was obtained with less inhibitory inputs relative to the amount of excitatory input (cf. parameter settings in Fig. 11). The resulting time course of membrane potential in the simulations is shown in Fig. 2 (right side) and the simulated relationship between the amplitude of the membrane potential and stimulus velocity is shown in Fig. 6B. The slope of the regression lines for the simulated responses of the nonspiking interneurons of types E1, E2, E3, E5, E6, and I2 showed only minor differences and are therefore represented by only one regression line. The same is true for the types E4 and I4. The regression lines of the simulation were always in the range of the experimental data. Minor differences in the physiology of simulated and real neurons are in the range of the physiological differences among individual animals.

The parameter "synaptic conductance" of the synapses onto a given nonspiking interneuron was therefore a result of the following prerequisites: (1) The overall response of the interneuron (depolarization or hyperpolarization) to elongation and relaxation stimuli has to be similar in simulation and reality; (2) The relationship between the amplitude of depolarization and hyperpolarization and the stimulus velocity has to correspond to the real neurons (see above); (3) The ratio between velocity component and position component in the response of the simulated neurons has to be the same as in the real neurons (compare with Fig. 2); (4) The time course of decay during the holding phase of the ramp-and-hold stimulus has to fit with values of the experimental data.

The passive membrane parameters of the simulation, i.e., membrane conductance and membrane capacitance, were set to values resulting from a time constant of about 50 ms, as measured by Driesang and Büschges (1993) for E4. In doing so, we assumed that the time constant is similar in all types of interneurons. No further active membrane properties, as, e.g., the voltage-dependent K^+ channels and Ca^{2+} channels as described in the locust (Laurent, 1990, 1991; Laurent et al. 1993), were introduced in the simulated nonspiking interneurons. This is, because as yet, there is no such experimental evidence for the existence of these channels in the individual identified nonspiking interneurons involved (see discussion).

*5. **Physiology of the Spiking Interneurons.*** From our experiments it was clear that nonspiking interneurons receive long latency inhibitory synaptic input from fCO signals (see above). We assumed that a group of spiking interneurons mediates the inhibition of the nonspiking interneurons, similar to the situation found in the locust (Burrows, 1987b). The physiology of these neurons could be deduced from experimental data (Driesang and Büschges, 1993; Sauer et al., 1995). The amplitude of hyperpolarization in the membrane potential of the nonspiking interneurons and the frequency of the IPSP's depended on stimulus velocity. Such properties of the spiking neurons in the simulation were chosen which fulfilled those assumptions (Table 1).

*6. **Response Characteristics of SETi.*** To obtain experimental data for the simulation parameters of "SETi" (Table 2) currents of different amplitudes were injected into this motoneuron during recordings from neuropilar processes. The resulting discharge rate of SETi was measured (Fig. 7). The passive parameters of "SETi" in the simulation were now chosen so that the relationship between current and spike-frequency in the simulation was in agreement with the experimental data (regression lines in Fig. 7). Thereby the absolute value of the spike frequency is of minor importance, because it depends in experiment and simulation on the distance between the site of current injection and the spike generating zone. In accordance with the spontaneous activity of SETi in the inactive animal (Bässler, 1983), the membrane potential of the simulated "SETi" was set to values just above the spike threshold.

The nonspiking interneurons described so far all provide synaptic drive to extensor motoneurons, that is,

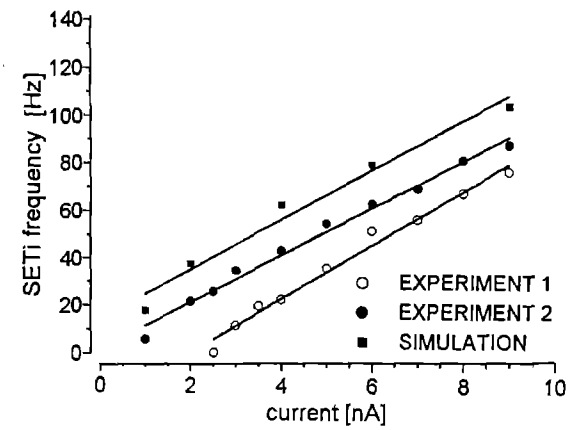

Figure 7. Relationship between the current injected into the SETi motoneuron and its mean discharge rate. Open and closed circles: experimental data from two different experiments; closed squares: data from the simulation. Note that the current in the simulation was injected into the third dendritic compartment according to the experimental application of the current injection at a location distant to the spike-generating zone.

also to SETi. In view of the physiological finding that only depolarizing current injections into the nonspiking interneurons of types E1, E2, E4, E5 (Büschges, 1990), E7, and I4 (this paper) affected SETi discharge rate, the resting membrane potential of these types of nonspiking interneurons in the simulation were set just below the threshold for transmitter release, that is, at about −50 mV (cf. Büschges, 1990; Driesang and Büschges, 1993) (Fig. 3B). For nonspiking interneurons of type I1 and I2 and for position-sensitive E-types, E2, E3, and E6, the resting membrane potential was above the threshold for transmitter release (Büschges, 1990) (see Table 1).

None of the interneurons has exactly the same response characteristics to fCO stimuli as SETi. The response characteristics of SETi therefore result from the summation of its inputs (see also Bässler, 1993). In a subsequent simulation it was tested whether the input to SETi from the 10 known types of nonspiking interneurons is quantitatively sufficient to induce the SETi response. The fixed simulation parameters were based on the physiological properties described above. This is true for the parameters for the simulation of the responses in the 10 nonspiking interneurons to rampwise stimulation (Table 1). The same is true for the parameters describing the output characteristics of the nonspiking interneurons. E-neurons excite SETi and I-neurons inhibit SETi. The parameter synaptic conductance of all synapses between E-neurons and SETi were set to the same value. The same was true for the synapses between I-neurons and SETi. Due to the experimental finding that changes of the SETi discharge rate upon hyperpolarizing and depolarizing currents injected into I-neurons has a steeper slope as in all investigated E-neurons (Büschges, 1990), the synaptic conductance between I-neurons and SETi is higher than the synaptic conductance between E-neurons and SETi (Fig. 11).

The simulation of the response of the SETi motoneuron to ramp-and-hold stimulation of the fCO had a satisfying result with all fixed simulation parameters when the coupling strengths of the synapses between the nonspiking interneurons and "SETi" were set for each E neurons approximately threefold lower (40 nS) than for each I type (130 nS) (compare Fig. 8A left and right). A quantitative comparison of the spike activity of the "simulated" and the "real" SETi motoneuron showed that the relationship between the activity and the stimulus velocity was similar in both cases (Fig. 8B).

7. Sensitivity of the Simulation Against Parameter Variation. In subsequent simulations we tested the influence of particular types of nonspiking interneurons on the overall SETi response. A simulation with a coupling strength of 65 nS between I1 and SETi (50% of the default coupling strength, marked as hyperpolarized in Fig. 9A) showed that the spike activity of the simulated SETi during rampwise relaxation of the fCO is not suppressed (Fig. 9A) as it is *in vivo* for this stimulus velocity. The same effect was obtained when I1 was kept hyperpolarized. We chose only 50% coupling strength in the simulation to mimic the hyperpolarization in the experiment because the effect of current injection into a neuron onto the output synapses varies, depending from the recording site.

The time course of SETi activity during a simulation in which the coupling of the simulated E3 was decreased to 50% (20 nS between E3 and SETi) is shown in Fig. 9B. In this case, spike activity of SETi during and after a stimulus was markedly decreased, as was also the case in experiments with E3 held hyperpolarized; 50% coupling of other interneuron types affected the motoneuronal output according to their complex physiology.

The most critical parameters in the simulation were the synaptic parameters conductance, synaptic delay and synaptic threshold. The parameter space of the conductance depended on the type of pre- and postsynaptic neuron. As such the synaptic connections to the nonspiking interneurons are relatively sensitive against minor changes. Increasing or decreasing the conductance of about 20% induced a dramatic change in the physiological properties of the nonspiking interneuron, that is, the dependency of membrane potential on a given stimulus parameter, such as stimulus velocity. The same was true for the parameter synaptic conductance. For synapses between nonspiking interneurons and SETi variation of this parameter up to 50% had only quantitative influences on the motoneuronal activity. This was shown above for type E3. For other types of interneurons, i.e., in particular neurons I1, I2, and I4, variation of this parameter had also qualitative effects on the result of the simulation. As such, with decreasing the synaptic conductance for the synapse between interneuron I1 and SETi, relaxation of the fCO no longer led to the inhibition of SETi during the fCO movement, normally typical for a given stimulus velocity.

Another critical parameter was the parameter synaptic delay. This was in particular true for the inhibitory

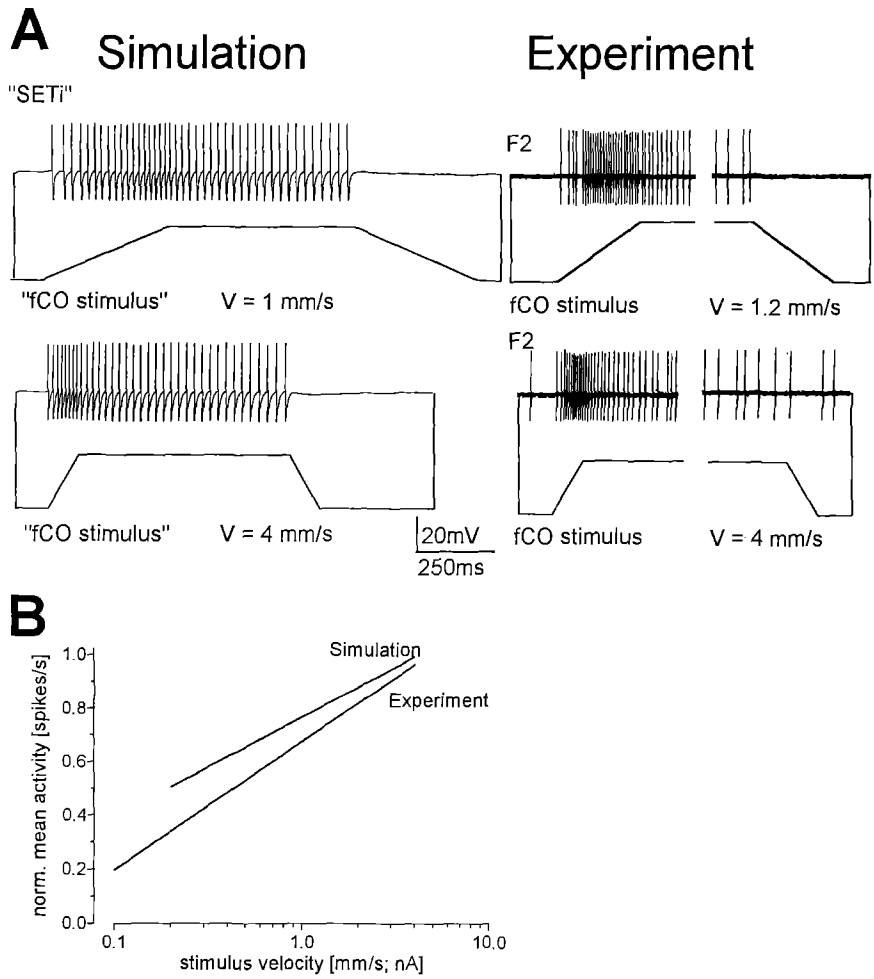

Figure 8. A. Motoneuronal output (SETi) of the simulated network in response to ramp-and-hold stimuli at the fCO. The spike activity of the simulation corresponds to a recording at the spike-generating zone of a "real" SETi. B. Plot of the SETi activity *versus* stimulus velocity. The responses of SETi of three animals were normalized. Note that the slope of the regression line of the experimental data resembles the experimental data to a high degree.

synapses between the spiking interneurons and non-spiking interneurons. The proper setting of this parameter results in the inhibition to be able to limit the depolarization induced by stimulus velocity. For that reason the minimum and maximum value for this parameter (Table 1) (10 ms and 22 ms) represents the limits for a realistic simulation.

Our simulation was based on the physiology of the neurons involved during rampwise stimuli. To further test our simulation, we applied sinusoidal stimuli to the simulated afferents and analyzed the SETi response. We compared the results of the simulation with data of experiments on *Cuniculina*, in which we applied a sinusoidal stimulus to the fCO (compare also with Bässler et al., 1982). Figure 10 shows that the simulated network produced a realistic SETi response. The spike activity of the SETi motoneuron in the simulation in response to different stimulus frequencies are in good agreement with the experimental data.

Discussion

The present paper describes a simulation of the posture control network of the stick insect femur-tibia (FT) joint in the inactive behavioral state, that is when the system generates resistance reflexes (Bässler, 1983). The simulation was based on empirical data on the

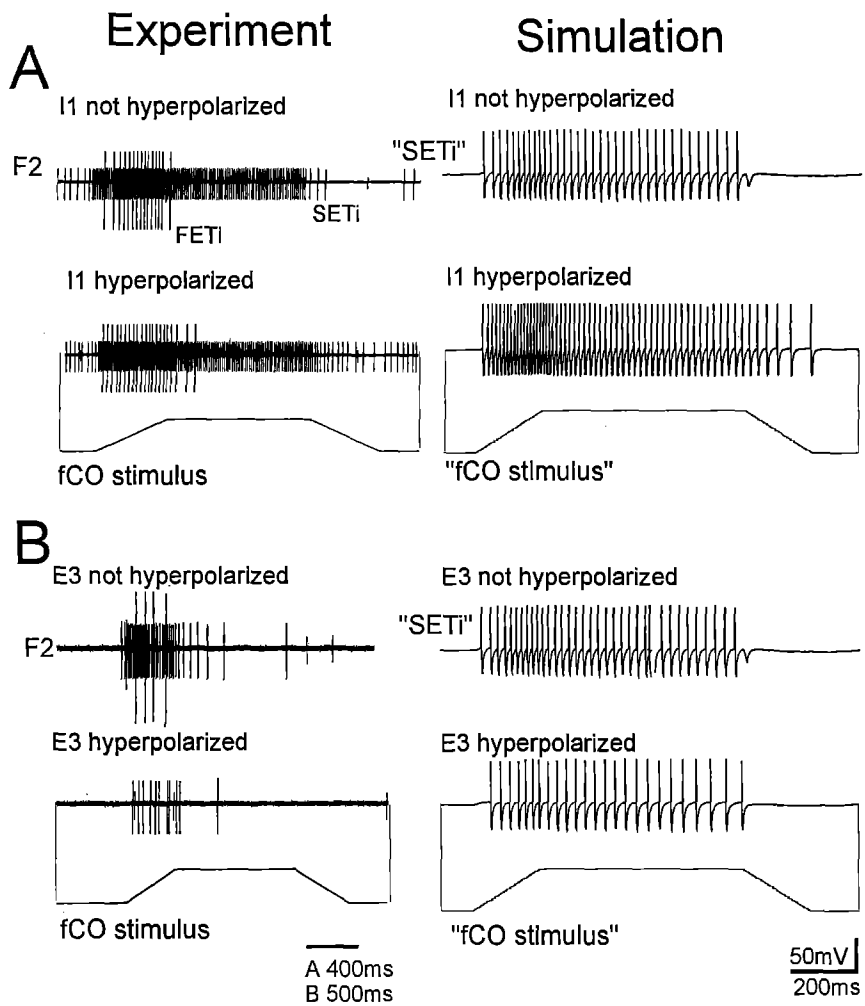

Figure 9. A. Effect of alteration in interneuronal membrane potential on motoroutput of FT control network. Simultaneous extracellular recording of the extensor nerve F2 (containing SETi, FETi, and CI_1) and intracellular recording of nonspiking interneuron I1 (not shown). The interneuron was either held at resting potential or it was hyperpolarized with −2 nA. For comparison, the output of the simulated network was shown in a simulation with 50% conductance of the synapse between interneuron I1 and SETi (details see text). Note that during relaxation stimuli there is no inhibition of SETi activity in the experiment and in the simulation with I1 hyperpolarized. B. Simultaneous recording from extensor nerve F2 and simultaneous intracellular recording from interneuron E3 (not shown). Hyperpolarizing this type of nonspiking interneuron in the experiment and 50% conductance of the synapse between interneuron E3 and SETi in the simulation led to a decrease in the SETi activity (see text).

neuronal elements of the joint control system. Four main results emerge from the success of the simulation:

- The characteristics of interneuronal responses to dynamic signals from the fCO can be explained by parallel excitatory and inhibitory inputs elicited by the movement parameter stimulus velocity plus input from adapting and nonadapting positions-sensitive fCO-units.
- The information currently available on this neuronal network is sufficient for a quantitative explanation of its motor output.
- The motor output of the neuronal network can be sufficiently explained by the action of parallel, distributed, and antagonistic pathways.
- The behavior of catalepsy can be sufficiently explained by this structure. It is one of the first behaviors that can be quantitative explained in a sufficient manner.

Topology of the Simulated Neuronal Network

Previous investigations have provided detailed knowledge of neuronal circuitry of sensory-motor pathways

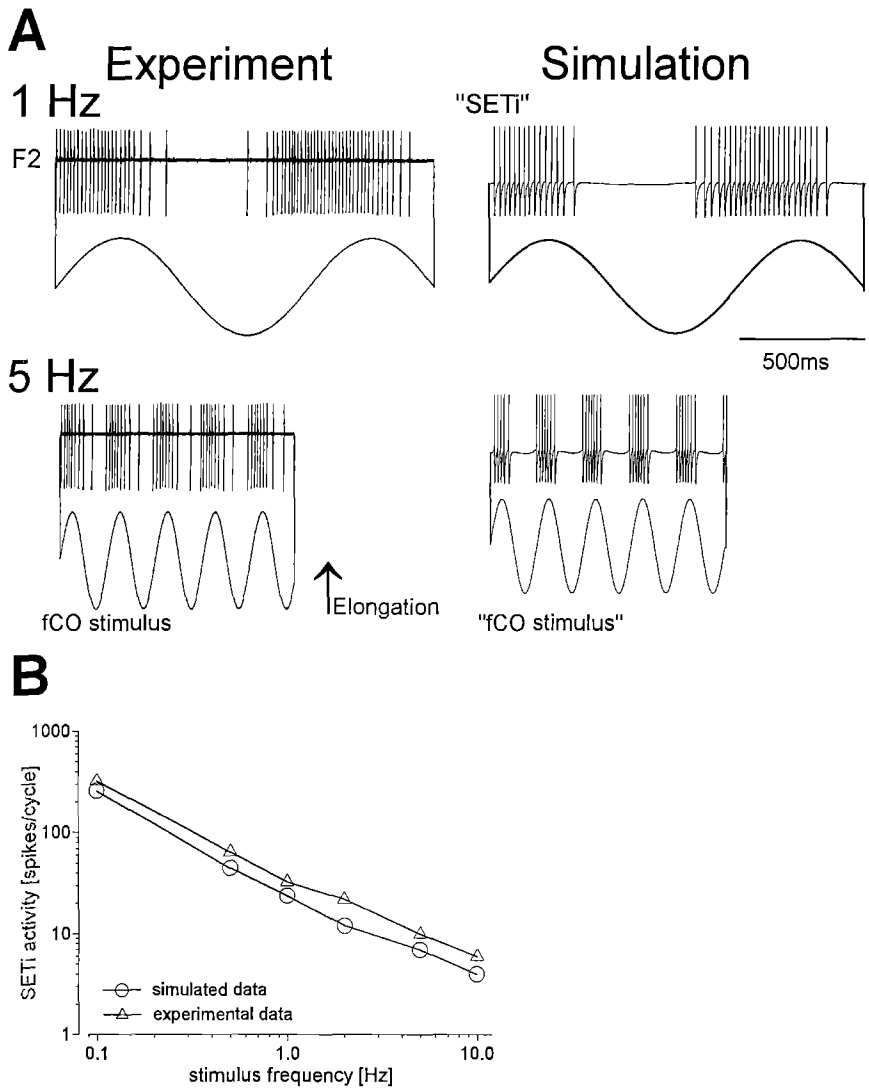

Figure 10. A. Comparison of the output of the simulated network and the experimental data with respect to the response of SETi to sinusoidal stimulation of the fCO (1 Hz and 5 Hz). B. The responses show the same characteristics with respect to the spike activity of the motoneuron.

controlling insect leg joints. Leg proprioceptors have been shown to project either directly (e.g., Pearson et al., 1976; Burrows, 1987a) or via intercalated interneurons, including spiking and nonspiking interneurons (e.g., Burrows et al., 1988; Burrows, 1989; Büschges, 1990) onto leg motoneurons. The same is true for projections from afferent neurons onto premotor interneurons (for summary see Burrows, 1992). Neuronal pathways transmitting a given stimulus parameter have been described as exclusively excitatory or exclusively inhibitory. However, Sauer et al. (1995) have shown that the nonspiking premotor interneurons of type E4, E5, and E6 in the femur-tibia control network of the stick insect receive parallel excitatory and inhibitory signals elicited by the same movement parameter stimulus velocity. Morphological and physiological evidence suggests that the excitatory signals are mediated by direct connections from fCO afferents, as is also known in the locust (Burrows et al., 1988), while inhibitory input is mediated by polysynaptic pathways via spiking interneurons (for a detailed discussion of connectivity, see Sauer et al., 1995). In the present investigation we have extended our knowledge on this kind of information processing to other interneurons in the control network that are depolarized by velocity signals during fCO movement, namely

interneurons of type E1, E2, E3, I2, and E7. The morphology of the intercalated spiking interneurons mediating the inhibition is not yet known, however. Further experiments are needed to determine whether local spiking interneurons known in the locust (Burrows, 1987b) are involved in mediating the inhibition.

The simulation has shown that with this network topology, the different responses of different types of nonspiking interneurons could be verified simply by changing the relative amount of excitation and inhibition. Thus, the different interneuronal physiology could be achieved using the same wiring scheme. It is quite conceivable that such a mechanism could also be involved in the generation and thus evolution of species-specific differences between homologous neurons *in vivo*. For example, the properties of FT control loops in other insect species are known to vary greatly (Bässler, 1983). As such, the femur-tibia control system of the locust middle leg, acting on the basis of the same principle of information processing and with most likely homologue interneurons, is much less velocity dependent than that of the stick insect (Ebner and Bässler, 1978; Büschges and Wolf, 1995).

Parliamentary Organization in Sensory-Motor Systems

The computer simulation showed that a neuronal network acting with parallel antagonistic pathways is sufficient to generate the resistance reflex of the inactive stick insect against passive leg movement. Bässler (1993) termed this information processing the *parliamentary principle*. In the generation of motor output during fCO elongation, that is, joint flexion, six E-type neurons and one I-type neuron support the overall resistance reflex (resisting influence) and one E-type (E7) and two I-type neurons (I2, I4) oppose it (assisting influence, Fig. 11A). During relaxation stimuli (joint extension) three E-type (E1, E2, E3) and all I-type neurons exert a resisting influence and four E-type neurons have an assisting influence (Fig. 11B). This network was capable of generating quantitatively the characteristics of the SETi following rampwise and sinusoidal stimulation of the fCO. Thus, in this network parallel antagonistic pathways interact on two levels: (1) at the input side of the premotor interneurons (see above) and (2) on the input side of the motoneurons. Recent results have indicated that a third level of interaction of antagonistic parallel pathways exists: presynaptic inhibition was found to act on the terminals of fCO afferents in the stick insect central nervous system. The activity of sensory signals from fCO afferents inhibits other afferents from the same sense organ (Sauer and Büschges, 1994), a mechanism previously investigated in detail in other invertebrate sensory-motor systems (Burrows and Laurent, 1993; Cattaert et al., 1992).

Network organizations using antagonistic parallel pathways have also been described for other joint control networks of insects (stick insect thoraco-coxal joint: Büschges and Schmitz, 1991; locust femur-tibia control network: Büschges and Wolf, 1995). They are also known in the generation of locomotion (Büschges et al., 1994; Wolf and Büschges, 1995). Similarly constructed neuronal networks have been described in other arthropods, such as in the uropod system of crayfish (Nagayama and Hisada, 1987; Namba et al., 1994), and in the neuronal network controlling the crayfish thoraco-coxal joint (Skorupski et al., 1992). This kind of information processing was also revealed in detailed studies of local bending reflexes in the leech (Lockery and Kristan, 1990a, b). There is also recent discussion that in *Aplysia* the neuronal network involved in the generation of the gill withdrawal reflex is organized similarly (Wu et al., 1994; Tsau et al., 1994; Frost and Kandel, 1995). Thus, it appears that information processing via parallel antagonistic pathways is not a specialization of posture control networks in insects. Instead it seems to be a general principle of network organization (see also Morton and Chiel, 1994).

The existence of antagonistic, parallel pathways could have another consequence concerning the flexibility of the network. The neuronal networks controlling vertebrates and invertebrate leg joints are state-dependent and phase-dependent on the motor output to a given stimulus (Pearson, 1993, 1995; Prochazka, 1989). For example, in the stick insect, the motor output in response to fCO signals can be reversed when the animal becomes active. This reflex reversal, called the active reaction (Bässler, 1976, 1988), is known to be an element of the walking motor pattern generation. Similar reflex reversals are present in other systems in invertebrates (Skorupski and Sillar, 1986) and vertebrates (Duysens et al., 1990). It is conceivable that a neuronal network with the topology described above could produce different motor outputs by changing the relative strengths of antagonistic pathways, an hypothesis that will be tested with the presented simulation.

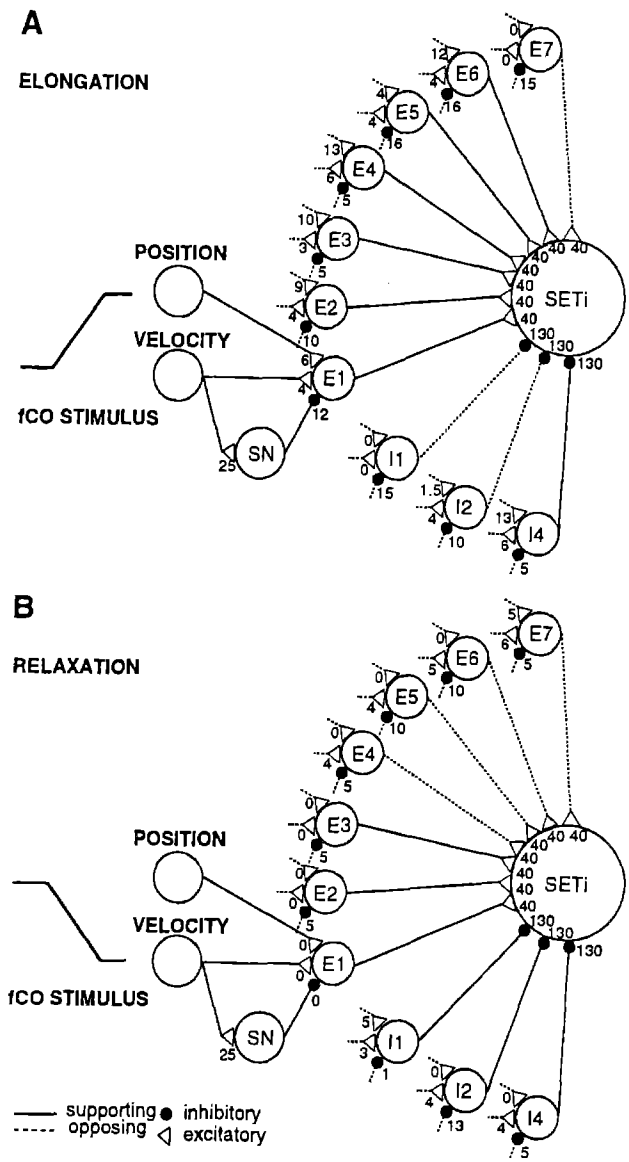

Figure 11. Schematic drawing of the neural circuit underlying the processing of sensory signals from the femoral chordotonal organ onto the extensor motoneurons used in the simulation presented in this paper. The basic connectivity of the network for each stimulus direction is shown separately (A. elongation; B. relaxation) to make the supporting and opposing contributions for each neuronal pathway more clear, the connections between the nonspiking interneurons and the motoneuron are represented by solid lines (supporting the generation resistance reflex) or dashed lines (opposing the generation of the resistance reflex). The network topology for fCO afferents, spiking interneurons and nonspiking interneurons is represented only once, each, although all nonspiking interneurons receive this same kind of input. The values for the parameter 'synaptic conductance' of the synapses were indicated beside each synapse (see text). (P^+ = position sensitive for elongation stimuli and P^- for relaxation stimuli, V^+ = velocity sensitive for elongation stimuli and V^- for relaxation stimuli.)

Validity of Simulation

Using a complex simulation tool like BioSim 4.3, one can nearly always obtain a solution for a given input-output relationship. Therefore a simulation is only a method of network analysis if stringent physiological constraints are introduced that limit the possible variables and if the assumptions of the simulation can be experimentally tested. The constraints were met in the present study by the physiology of the

afferents, the connections from afferents onto nonspiking interneurons, the physiology of the nonspiking interneurons and the connections from the nonspiking interneurons onto the motoneurons. Most of the assumptions that led to a successful simulation are experimentally testable.

The parameters for the simulation not directly known from physiological experiments were (1) the existence of the spiking neurons mediating inhibition of nonspiking interneurons. (2) The relative weighting of the synapses of all E- or I-type neurons. (3) The absolute values of the synaptic conductance, like the strengths of the connections between the nonspiking interneurons and the motoneuron. (4) The connections between nonspiking interneurons and SETi being mono- or polysynaptically. The values for the parameters concerning these physiological data are therefore not quantitatively known and are thus only a rough estimate.

Compared to the extensive knowledge about physiological properties of spiking and nonspiking neurons in insects (Laurent, 1990), the simulation of these neurons appears to be a simplification. Nonspiking interneurons were simulated as though they were only passive elements. Thus, the simulation used a paradigm that at first glance contrasts the recent findings that nonspiking interneurons exhibit voltage-dependent active membrane properties (Laurent, 1990, 1991; Laurent et al., 1993). However, we did not introduce these properties, that is the outward rectification of the membrane potential, for several reasons:

- Voltage clamp measurements on nonspiking interneurons of type E4 by Driesang and Büschges (1993) during resistance reflex activation have given no evidence that the above described properties play a role within the range of membrane potentials generated in this behavioral context.
- The time course of the membrane potential in SETi depends only on the stimulus velocity and not on the amplitude of membrane depolarization as it would have to be expected in case of outward rectification in the premotor neurons playing a crucial role (cf. Fig. 12 in Bässler, 1993).
- Preliminary simulations showed that introducing outward rectification by the interneurons had a comparable effect on the time course of membrane potential as the delayed inhibition via intercalated spiking interneurons. As the latter mechanisms in contrast to the previous one is known to be existent for the individual identified neurons simulated, we have incorporated only him in the simulation.

Nevertheless, the neuronal elements in the simulation are able to produce the input-output relationships known from real neurons. These characteristics were (1) the direction of the change of the membrane potential in the neuron as the response to the fCO stimuli, (2) the ratio of velocity component and the position component in the interneuronal response, (3) the latencies between fCO stimulus and interneuronal responses, (4) the relationship between amplitude of the neuronal response and stimulus velocity, and (5) the time constants of decay in the membrane potential during the holding phase of the rampwise stimulus.

Despite current knowledge about presynaptic inhibition of sensory afferents we did not introduce this mechanism in our simulation by now. Evidence was presented that this mechanism might contribute to modulations in gain of reflex responses (Burrows and Matheson, 1994). However, preliminary simulations demonstrated that its implementation is not necessary for simulating the motor response in inactive animals as long as changes in gain are not intended (A. Sauer, unpublished). Perhaps its incorporation is necessary when the realization of gain changes (Kittmann, 1991; Bässler and Nothof, 1994) or reflex reversals (Bässler, 1986; Driesang and Büschges, 1996) is intended.

Acknowledgments

We thank Drs. Joachim Schmidt and Siglinde Gramoll for many stimulating discussions and their comments on this manuscript. In addition, we thank two anonymous referees for their valuable suggestions on the manuscript. We are indebted to Mary Anne Cahill for correcting the English text. This work was supported by DFG-grants Ba 578 and Bu 857.

References

Anastasio TJ, Robinson DA (1990) Distributed parallel processing in the vertical vestibulo-ocular reflex: Learning networks compared to tensor theory. *Biol. Cybern.* 63:161–167.

Bässler U (1976) Reversal of a reflex to a single motoneuron in the stick insect *Carausius morosus*. *Biol. Cybern.* 24:47–49.

Bässler U (1983) Neural basis of elementary behavior in stick insects. Springer Verlag, Berlin.

Bässler U (1986) Afferent control of walking movements in the stick insect *Cuniculina impigra*. II. Reflex reversal and the release of swing phase in the restrained foreleg. *J. Comp. Physiol.* A158:351–362.

Bässler U (1988) Functional principles of pattern generation for walking movements of stick insects forelegs: The role of the femoral chordotonal afferences. *J. Exp. Biol.* 136:125–147.

Bässler U (1993) The femur-tibia control system of stick insects: A model system for the study of the neural basis of joint control. *Brain Research Reviews* 18:207–226.

Bässler U, Storrer J, Saxer K (1982) The neural basis of catalepsy in the stick insect *Cuniculina impigra*. 2. The role of the extensor motor neuron and the characteristic of the extensor tibiae muscle. *Biol. Cybern.* 46:1–6.

Bässler U, Hofmann T, Schuch U (1986) Assisting components within a resistance reflex of the stick insect, *Cuniculina impigra*. *Physiol. Entomol.* 11:359–366.

Bässler U, Büschges A (1990) Interneurones participating in the "active reaction" in stick insects. *Biol. Cybern.* 62:529–538.

Bässler U, Nothof U (1994) Gain control in a proprioceptive feedback loop as a prerequisite for working close to instability. *J. Comp. Physiol.* A174:23–33.

Bergdoll S, Koch UT (1995) BIOSIM: A biological neural network simulator for research and teaching, featuring interactive graphical user interface and learning capabilities. *Neurocomputing* 8:93–112.

Büschges A (1990) Nonspiking pathways in a joint-control loop of the stick insect *Carausius morosus*. *J. Exp. Biol.* 151:133–160.

Büschges A (1994) The physiology of sensory cells in the ventral scoloparium of the stick insect femoral chordotonal organ. *J. Exp. Biol.* 189:285–292.

Büschges A, Schmitz J (1991) Nonspiking pathways antagonize the resistance reflex in the thoraco-coxal joint of stick insects. *J. Neurobiol.* 22:224–237.

Büschges A, Kittmann R, Schmitz J (1994) Identified nonspiking interneurons in leg reflexes and during walking in the stick insect. *J. Comp. Physiol.* A 174:685–700.

Büschges A, Wolf H (1995) Nonspiking local interneurons in insect leg motor control. I. Common layout and species-specific response properties of femur-tibia joint control pathways in stick insect and locust. *J. Neurophysiol.* 73:1843–1860.

Burrows M (1987a) Parallel processing of proprioceptive signals by spiking local interneurons and motor neurones in the locust. *J. Neurosci.* 7:1064–1080.

Burrows M (1987b) Inhibitory interactions between spiking and nonspiking local interneurons in the locust. *J. Neurosci.* 7:3282–3292.

Burrows M (1989) Processing of mechanosensory signals in local reflex pathways of the locust. *J. Exp. Biol.* 146:209–227.

Burrows M (1992) Local circuits for the control of leg movement in an insect. *TINS* 15:226–232.

Burrows M, Laurent GJ, Field LH (1988) Proprioceptive inputs to nonspiking local interneurons contribute to local reflexes of a locust hindleg. *J. Neurosci.* 8:3085–3093.

Burrows M, Laurent GJ (1989) Reflex circuits and the control of movement. In: R Durbin, C Miall, G Mitchison, eds. The Computing Neuron. Addison-Wesley Publishing Co., Wokingham. pp. 244–261.

Burrows M, Laurent GJ (1993) Synaptic potentials in the central terminals of locust proprioceptive afferents. *J. Neurosci.* 13:808–819.

Burrows M, Matheson, T (1994) A presynaptic gain control mechanism among sensory neurons of a locust leg proprioceptor. *J. Neurosci.* 14:272–282.

Cattaert D, El Manira A, Clarac F (1992) Direct evidence for presynaptic inhibitory mechanisms in crayfish sensory afferents. *J. Neurophysiol.* 67:610–624.

Driesang RB, Büschges A (1993) The neural basis of catalepsy in the stick insect. IV. Properties of nonspiking interneurons. *J. Comp. Physiol.* A 173:445–454.

Driesang RB, Büschges A (1996) Physiological changes in central neuronal pathways contributing to the generation of a reflex reversal. *J. Comp. Physiol.* A, in press.

Duysens J, Trippel M, Horstmann GA, Dietz V (1990) Gating and reflex reversal of reflexes in ankle muscles during human walking. *Exp. Brain. Res.* 82:351–358.

Ebner I, Bässler U (1978) Zur Regelung der Stellung des Femur—Tibia Gelenks im Mesothorax der Wanderheuschrecke *Schistocerca gregaria* (Forskal). *Biol. Cybern.* 29:83–96.

Egelhaaf M, Borst A (1993) Motion computation and visual orientation in flies. *Comp. Biochem. Physiol.* 104A:659–673.

El Manira A, Cattaert D, Clarac F (1991) Monosynaptic connections mediate resistance reflex in crayfish (*Procambarus clarkii*) walking legs. *J. Comp. Physiol.* A168:337–349.

Frost WN, Kandel ER (1995) Structure of the network mediating siphon-elicited siphon withdrawal in *Aplysia*. *J. Neurophysiol.* 73:2413–2427.

Grimm K, Sauer AE (1995) The high number of neurons contributes to the robustness of the locust flight-CPG against parameter variation. *Biol. Cybern.* 72:329–335.

Harris-Warrick RM, Nagy F, Nusbaum MP (1992a) Neuromodulation of stomatogastric networks by identified neurons and transmitters. In: RM Harris-Warrick, E Marder, AI Selverston, M Moulins, eds. Dynamic Biological Networks: The Stomatogastric Nervous System, MIT Press, Boston. pp. 87–137.

Harris-Warrick RM, Marder E, Selverston AI, Moulins M, eds. (1992b) Dynamic Biological Networks. The Stomatogastric Nervous System. MIT Press, Cambridge, Mass.

Hofmann T, Koch UT (1985) Acceleration receptors in the femoral chordotonal organ of the stick insect, *Cuniculina impigra*. *J. Exp. Biol.* 114:225–237.

Hofmann T, Koch UT, Bässler U (1985) Physiology of the femoral chordotonal organ in the stick insect, *Cuniculina impigra*. *J. Exp. Biol.* 114:207–223.

Kittmann R (1991) Gain control in the femur-tibia feedback system of the stick insect. *J. Exp. Biol.* 157:503–522.

Laurent G (1990) Voltage-dependent nonlinearities in the membrane of locust nonspiking local interneurons, and their significance for synaptic integration. *J. Neurosci.* 10:2268–2280.

Laurent G (1991) Evidence for voltage-activated outward currents in the neuropilar membrane of locust nonspiking interneurons. *J. Neurosci.* 11:1713–1726.

Laurent G, Seymour-Laurent KJ, Johnson K (1993) Dendritic excitability and a voltage-gated calcium current in locust nonspiking local interneurons. *J. Neurophysiol.* 69:1484–1498.

Lockery SR, Kristan WB (1990a) Distributed processing of sensory information in the leech. I. Input-output relations of the local bending reflex. *J. Neurosci.* 10:1811–1815.

Lockery SR, Kristan WB (1990b) Distributed processing of sensory information in the leech. II. Identification of interneurons contributing to the local bending reflex. *J. Neurosci.* 10:1816–1829.

Matheson T (1992) Range fractionation in the locust metathoracic femoral chordotonal organ. *J. Comp. Physiol.* A170:509–520.

McClelland JL, Rumelhart DE (1988) Parallel Distributed Processing. MIT Press, Cambridge, Mass.

Morton D, Chiel H (1994) Neural architectures for adaptive behavior. *TINS* 17:413–420.

Nagayama T, Hisada T (1987) Opposing parallel connections through crayfish local nonspiking interneurons. *J. Comp. Neurol.* 257:347–358.

Namba H, Nagayama T, Hisada M (1994) Descending control of nonspiking local interneurons in the terminal abdominal ganglion of the crayfish. *J. Neurophysiol.* 72:235–247.

Osborn CE, Popelle RE (1992) Parallel distributed network characteristics of the DSCT. *J. Neurophysiol.* 68:1100–1112.

Pearson KG (1993) Common principles of motor control in vertebrates and invertebrates. *Ann. Rev. Neurosci.* 16:265–297.

Pearson KG (1995) Reflex reversal in the walking systems of mammals and arthropods. In: WR Ferrell, U Proske, eds. Neural Control of Movement. Plenum Press, New York. pp. 135–141.

Pearson KG, Wong RKS, Fourtner CR (1976) Connexions between hair-plate afferents and motoneurons in the cockroach leg. *J. exp. Biol.* 64:251–266.

Pearson KG, Ramirez JM (1992) Parallels with other invertebrate and vertebrate motor systems. In: RM Harris-Warrick, E Marder, AI Selverston, M Moulins, eds. Dynamic Biological Networks: The Stomatogastric Nervous System. MIT Press, Cambridge, MA.

Prochazka A (1989) Sensorimotor gain control: A basic strategy of motor systems? *Prog. Neurobiol.* 33:281–307.

Ritzmann RE, Pollack AJ (1990) Parallel motor pathways from thoracic interneurons of the ventral giant interneuron system of the cockroach *Periplaneta americana*. *J. Neurobiol.* 21:1219–1235.

Rudomin P (1990) Presynaptic inhibition of muscle spindle and tendon organ afferents in the mammalian spinal cord. *Trend Neurosci.* 13:499–505.

Sauer AE, Büschges A (1994) Presynaptic inhibition of afferents—A mechanism influencing gain in proprioceptive feedback systems. In: N Elsner, H Breer, eds. Götingen Neurobiology Report 1994. Georg Thieme Verlag Stuttgart, New York. p. 283.

Sauer AE, Driesang RB, Büschges A, Bässler U (1995) Information processing in the femur-tibia control loop of stick insects 1. The response characteristics of two nonspiking interneurons result from parallel excitatory and inhibitory inputs. *J. Comp. Physiol.* A177:145–158.

Schmitz J, Delcomyn F, Büschges A (1991) Oil and hook electrodes for en passant recording from small nerves. In: PM Conn, ed. Methods in Neuroscience 4. Academic Press, San Diego. pp. 266–278.

Shepherd GM (1988) Neurobiology. 2nd ed. Oxford University Press, New York.

Skorupski P, Rawat BM, Bush BMH (1992) Heterogenity and central modulation of feedback reflexes in crayfish motor pool. *J. Neurophysiol.* 67:648–663.

Skorupski P, Sillar KT (1986) Phase-dependent reversal of reflexes mediated by the thoracocoxal muscle receptor organ in the crayfish, *Pacifastacus leniusculus*. *J. Neurophysiol.* 55:689–695.

Tsau Y, Wu J-Y, Hopp H-P, Cohen LB, Schiminovich D, Falk CX (1994) Distributed aspects of the response to siphon touch in *Aplysia*: spread of stimulus information and cross-correlation analysis. *J. Neurosci.* 14:4167–4184.

Weiland G, Koch UT (1987) Sensory feedback during active movements of stick insects. *J. Exp. Biol.* 133:137–156.

Wendel O (1993) MOBIS: Ein wissensbasiertes Experimentiersystem zur Simulation biologisch orientierter neuronaler Netze. In: R Hofestädt, F Krückerberg, T Lengauer, eds. Informatik in den Biowissenschaften. Springer-Verlag, Berlin. pp. 203–213.

Wolf H (1991) Sensory feedback in the locust flight patterning. In: DM Armstrong, BMH Busch, eds. Local Neuronal Mechanism in Arthropods and Vertebrates. Manchester University Press, Manchester. pp. 134–148.

Wolf H, Büschges A (1995) Nonspiking local interneurons in insect local motor control. 2. The role of nonspiking local interneurons in the control of leg swing during walking. *J. Neurophyiol.* 73:1861–1875.

Wu J-Y, Cohen LB, Falk CX (1994) Neuronal activity during different behaviors in *Aplysia*: A distributed organization? *Science* 263:820–823.

Zecevic D, Wu J-Y, Cohen LB, London JA, Höpp H-P, Falk CX (1989) Hundreds of neurons in the *Aplysia* abdominal ganglion are active during the gill-withdrawal reflex. *J. Neurosc.* 9:3681–3689.